

INFLUENCE OF CONTROL POWER RATE ON HIGH-ALPHA ROLL MANOEUVRABILITY

Philip Månsson¹

¹Saab Aeronautics, Linköping, Sweden

Abstract

To achieve high manoeuvre performance in unstable aircraft, it is essential to ensure proper stabilisation, agility and excellent flying and handling qualities (FQ/HQ). Traditional sizing methods for control power seldom include the aspects of control power rate for FQ/HQ. Sizing of control power rate is critical for ensuring excellent FQ/HQ and necessitates a sizing approach that allows sufficiently rapid manoeuvre onset, precision tracking and attitude control. This paper exemplifies the impact of control power rate on achieving MIL-STD flying qualities level (FQL) for a specific fighter aircraft concept, with a particular focus on high angle of attack roll performance. Analyses highlight the necessity of adequate control power rate and the impact of thrust vectoring. Additionally, roll manoeuvrability in the particularly demanding post-stall regime is also demonstrated with thrust vectoring.

Keywords: Control power rate, control surface deflection rate, roll performance, thrust vectoring

1. Introduction

Within the Saab Future Combat Air System (FCAS) programme, there is a continuous exploration of new concepts and evaluation of their operational effectiveness across different scenarios. The maturity level of each concept varies, depending on the purpose of study. Manned and unmanned aircraft are both studied as part of the project. In this investigation, a concept for a supersonic fighter aircraft has been used as a test model.

Significant design challenges are presented for flying vehicles with a large range in both flight and manoeuvre envelope. Comprehensive understanding of interdisciplinary trade-off studies is necessary to increase the design balance earlier in the conceptual design phase [1]. Platforms requiring high stability augmentation, agility and flying/handling qualities (FQ/HQ) demand early integration of flight dynamics in the design phase. This need is accentuated when the platform aerodynamics exhibit nonlinear characteristics at high-incidence flight conditions, and control effectors require complex control allocation to realize maximum manoeuvre performance. Notably, aircraft designed for low observability (i.e., 'stealth') can introduce such additional complexities. The stability and control characteristics that are sought for ensuring high manoeuvrability, flight safety and keeping project risk low are therefore stressed.

To ensure mission capabilities from a flight controls perspective, requirements are broken down into desired manoeuvre performance to ensure mission effectiveness and flight safety. Manoeuvre envelope can be specified in terms of angle of attack range, load factor, roll rate, sideslip angle whilst meeting handling qualities targets. Handling qualities targets with a pilot in the loop imply certain response characteristics for suitable 'feel' and control while piloting the platform.

The flight mechanics tasks during the conceptual design phase involve sizing of control power so that a permissible centre of gravity range can be established from a flight mechanics standpoint. Additionally, the design choices must also cater for the possibility to achieve desirable FQ/HQ whilst meeting

manoeuvre and trim design targets. Ensuring excellent FQ/HQ necessitates a sizing approach that allows sufficiently rapid manoeuvre onset and adequate tracking capability. Consideration must be given to control saturation in terms of deflection and rate limits such that stabilisation and handling is not degraded. MIL-STDs-1797 specify max roll time constants or time-to-bank angle change which include such response quality and are rated versus flying qualities levels [2]. Ultimately, handling qualities evaluation needs to be performed with pilot-in-the-loop simulators or flight tests to include important elements such as stick forces, command shaping, visual cues, motion cues and more.

To analyse the required control power rate, it is necessary to study both the demands of stabilisation due to external disturbances and manoeuvring as well as the combination thereof. This is further stressed when having to consider carefree or load-limiting handling of the platform for aggressive piloting. In the case of inherently unstable platforms, the stabilising function of the control system requires some budget of the available control power, imposing greater constraints when combined with manoeuvring demands.

2. Flight Control Model

The flight control model is developed within the Saab Future Combat Air System (Saab FCAS) project. Manned and unmanned aircraft are studied as part of the project. A concept for a supersonic fighter aircraft has been used as a test model in this investigation.

During the concept development phase of a new aircraft, it is of particular interest to increase the knowledge and design freedom earlier in the design process. This has been done by utilising several models and scaling functions to approximate different design solutions. This requires the FCS model to readily handle variations of the design with automatic updating of the control laws.

Flight dynamics analyses are conducted with a 6-DoF nonlinear simulation tool. The aerodynamic model for this concept aircraft has been created using both CFD simulation and low speed wind tunnel testing, see figure 1. The coverage is provided over a feasible flight and manoeuvre envelope which excludes extrapolation from the aero data set. Within the high-alpha region, the data set contains more uncertainties.



Figure 1 – Saab FCAS concept fighter in the L-2000 Wind tunnel at KTH.

With mass and inertia data from the CAD model and a preliminary engine model for the engine thrust it is possible to create a complete aircraft model useful for flight dynamics simulation. The model can then be used to evaluate manoeuvre or mission requirements as illustrated in Figure 2.

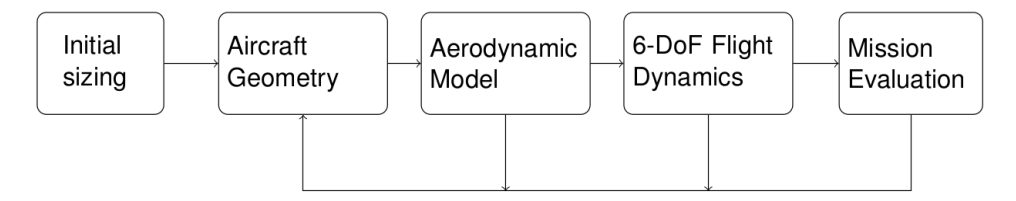


Figure 2 – Flight dynamics in the conceptual design phase.

The flight control system (FCS) model performs automatic generation of control laws based on the stability and control characteristics of the concept as well as inputs from other models such as inertia and actuation. Desired manoeuvre and FQ targets are specified in the FCS. The gain scheduling and control allocation is solved at runtime using an NDI-based formulation and allows close to maximum achievable manoeuvre performance. The concept has six control surfaces which can be scheduled to provide control power around all aircraft axes together with an optionally vectored thrust.

It is desirable to be able to keep key design parameters flexible for as long as possible in the design process to find the best overall design for the mission requirements. In order to reduce the number of full design iterations where model updates are necessary, the flight dynamics tool incorporates models for several design parameters. In this case, many of the aircraft properties are parameterised such that design changes can be applied at runtime in simulations. Examples of these properties are:

- Position of centre of gravity
- Moments of inertia
- Airframe inherent stability
- Available control power about all axes
- Control surface deflection rate
- Manoeuvre authority

The manoeuvre authority refers to the model reference parameters within the command shaping part of the FCS. These include the manoeuvre and responsiveness targets. Examples of those parameters are time constants for changes in commanded angular rate and limits for the maximum allowed roll rate and load factor.

2.1 Control surface scaling function

The control power and control power rate are varied by specifying control surface configuration, size, max deflection range and deflection rate. This is achieved using a model that generates scaling factors, which are used to scale the associated aerodynamic coefficients. These in turn update the control laws. The scaling can be done either explicitly or through geometric definition, by which it is possible to scale, add/remove and position the control surfaces. The scaling model is constrained by the outline of the planform. Thus, the resized control surfaces will not affect the airframe stability coefficients and require an update of the aerodynamic model. The FCS accounts for the reconfigured control power and the number of control surfaces within the simulation environment.

2.2 Thrust vector control model

The thrust vector control (TVC) has been modelled similar to a control surface with limits on rate and deflection. The vectoring is commanded through two different input signals to steer in pitch, $\delta_{TV,P}$ and yaw $\delta_{TV,Y}$. The limit of the deflections to steer in pitch and yaw are determined by the combined deflection in relation to the maximum allowed angular deviation from the axial line of the engine, $\theta_{TV,MAX}$. Default values for the following thrust vectoring parameters have been set to:

- $\theta_{TV,MAX}$ =20deg
- F_{TV.LIM}=12000N

 $\theta_{TV,MAX}$ depends on the maximum allowed radial force of the engine, $F_{TV,LIM}$, which is used to model a structural limit. Application of high engine thrust can reduce the max allowed deflection to respect $F_{TV,LIM}$. Both the $\theta_{TV,MAX}$ and $F_{TV,LIM}$ are parametrised to be able to conduct design trade-off studies.

3. Control power rate

This study examines the impact of the control power rate, which is the rate at which the control moment builds up. This is evaluated on the achievable manoeuvre performance with respect to agility and FQ/HQ. The control power is the control moment, denoted as M_{ctrl} , resulting from control surface deflection, δ_{ctrl} , expressed by equation 1. Control power rate is expressed as the moment build-up rate, \dot{M}_{ctrl} , due to control surface deflection rate, $\dot{\delta}_{ctrl}$, expressed by equation 2, derived with the assumption of constant Q and $Cm_{\delta_{ctrl}}$.

$$M_{ctrl} [Nm] = Q \cdot S \cdot l \cdot Cm_{\delta_{ctrl}} \cdot \delta_{ctrl}$$
 (1)

$$\dot{M}_{ctrl} [Nm/s] = Q \cdot S \cdot l \cdot Cm_{\delta_{ctrl}} \cdot \dot{\delta}_{ctrl}$$
 (2)

Here, M_{ctrl} represents the control moment for a specific control axis (pitch, roll, yaw). Q, is the dynamic pressure, S, the wing reference area, l, a wing reference length and $Cm_{\delta_{ctrl}}$, the control effectiveness derivative for the corresponding control axis.

The size of a control surface affects both the control power and the control power rate through $Cm_{\delta_{ctrl}}$. Consequently, the control power rate is more readily handled through the deflection rate of a control surface, $\dot{\delta}_{ctrl}$. Control power rate therefore depends on the product of $Cm_{\delta_{ctrl}} \cdot \dot{\delta}_{ctrl}$, as the primary design parameters.

For platforms where control power (control surface size and deflection range) cannot be further increased - either due to inherent design challenges specific to the chosen configuration or an inadequate design balance among different disciplines such as loads, structures design, actuator design, the required rate with respect to FQ/HQ becomes more critical. This must also be considered for various failure cases. Previous experiences at Saab in sizing of control power and rate have encompassed meeting several FQ/HQ targets, Pilot-induced Oscillation (PIO) resistance, failure transients, all weather operations, including scenarios with cold hydraulic fluid at extreme negative temperatures.

From a flight dynamics perspective, normalising equations 1 and 2 with moment of inertia, I, proves more useful in quantifying control power and rate:

$$M_{ctrl}/I = \dot{\omega}_{ctrl}[rad/s^2] \tag{3}$$

$$\dot{M}_{ctrl}/I = \ddot{\omega}_{ctrl}[rad/s^3] \tag{4}$$

Here, $\dot{\omega}_{ctrl}$ represents angular acceleration and $\ddot{\omega}_{ctrl}$ represents angular jerk for the corresponding control axis. The angular jerk is also referred to as the acceleration build-up rate. As an example on the use of the normalised quantity, $\dot{\omega}_{ctrl}$ - sizing of pitch control power involves achieving sufficient pitch acceleration, \dot{q} , to ensure adequate nose-down authority from a high-incidence flight condition [3]. The normalised quantities are used to denote the terms control power and control power rate.

3.1 Stability Axis Roll

For fighter aircraft manoeuvring at high angles of attack (AoA), rolling is typically controlled around the stability axis of the aircraft, aligning with the velocity vector for zero angle of sideslip (AoS). Figure 3 illustrates how the aircraft rolls around the stability axis. By using such control variable in roll, the effective roll control is facilitated due to that the angle of sideslip is regulated to minimise the coupling dynamics between axes. For example, the strong Cl_{β} -effect (rolling moment due to sideslip) of delta shaped planforms can contaminate roll response and cause undesirable cross-coupling that may adversely affect pilots' opinion about the FQ/HQ.

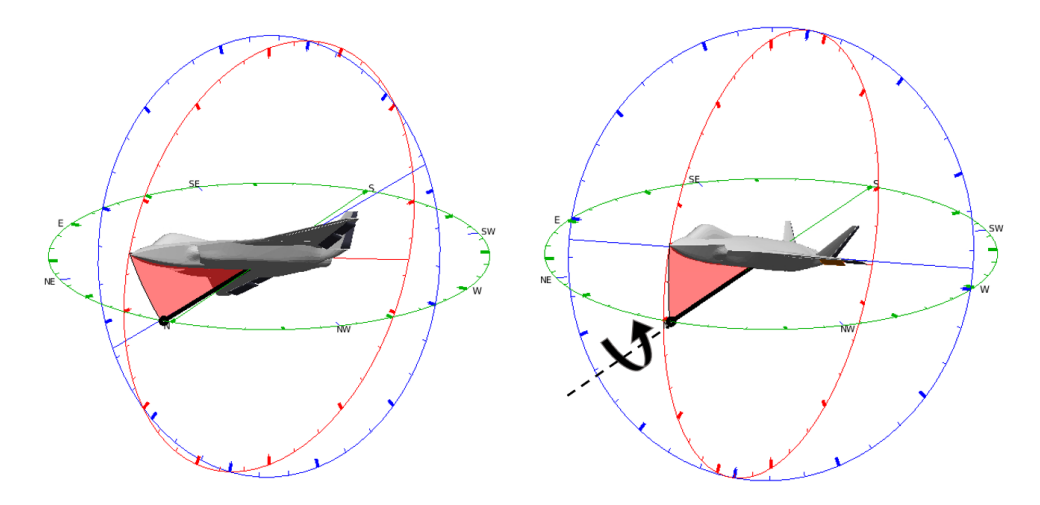


Figure 3 – Stability axis roll at high α . The excursion in AoS is minimised during the manoeuvre.

Insight into the required control power rates for this manoeuvre is provided by examining the kinematic equations for stability vector roll rate, p_s as given by equation 5, and the stability vector yaw rate, r_s , as given by equation 6. Note that r_s the is the simplified $\dot{\beta}$ -equation, excluding attitude and translational acceleration terms.

$$p_s \left[rad/s \right] = p_b cos(\alpha) + r_b sin(\alpha) \tag{5}$$

$$\dot{\beta}[rad/s] = -r_s = p_b sin(\alpha) - r_b cos(\alpha)$$
 (6)

These are expressed in terms of body referenced roll rate, p_b and yaw rate, r_b . As seen in equation 5, a combination of body axis roll and yaw rate is required to rotate around the stability vector. Typically for delta configurations, roll performance at high AoA is limited due to insufficient yaw control power from the vertical control surfaces to coordinate the turn and maintain a small angle of sideslip. Further insight is given by differentiating 6 with respect to time to yield β , as shown in equation 7.

$$\ddot{\beta} = \dot{p}_b sin(\alpha) - \dot{r}_b cos(\alpha) + \dot{\alpha} [p_b cos(\alpha) + r_b sin(\alpha)] \tag{7}$$

By noticing that the bracketed term is equal to equation 5, and assuming roll coordination both in onset as well as steady state, such that $\dot{\beta} = \ddot{\beta} = 0$, it is possible to derive an expression for the required control power in yaw, $\dot{r}_{b_{rea}}$:

$$\dot{r}_{b_{rea}} = \dot{p}_b tan(\alpha) + \dot{\alpha} p_s / cos(\alpha) \tag{8}$$

This equation indicates that high yaw control power is necessary for achieving high roll acceleration at high α as well as for high roll rates, p_s , in combination with positive dynamic manoeuvring in pitch, involving $\dot{\alpha}$.

A similar expression can be derived for the required yaw control power rate, $\ddot{r}_{b_{req}}$, by differentiating equation 7, giving $\ddot{\beta}$, and assuming that the acceleration build-up is also coordinated such that $\dot{\beta} = \ddot{\beta} = \ddot{\beta} = 0$.

$$\ddot{r}_{b_{rea}} = \ddot{p}_b tan(\alpha) + 2\dot{\alpha}\dot{p}_s/cos(\alpha) + \ddot{\alpha}p_s/cos(\alpha)$$
(9)

Equation 9 shows that high yaw control power rate is necessary for achieving fast response in stability vector roll at high α and more so when the manoeuvring is transient in pitch through the $\dot{\alpha}$ -, $\ddot{\alpha}$ -terms.

Simplifying further by excluding any dynamics in pitch, such that $\dot{\alpha} = \ddot{\alpha} = 0$, gives the simple relationship in control power rate for angle of sideslip regulation during a stability axis roll with constant load factor:

$$\ddot{r}_b/\ddot{p}_b = tan(\alpha) \tag{10}$$

In a similar fashion, taking the double derivative of p_s , equation 5, yields:

$$\ddot{p}_{s} = \ddot{p}_{b}cos(\alpha) + \ddot{r}_{b}sin(\alpha) + 2\dot{\alpha}[\dot{r}_{b}cos(\alpha) - \dot{p}_{b}sin(\alpha)] - \dot{\alpha}^{2}[p_{b}cos(\alpha) + r_{b}sin(\alpha)] - \ddot{\alpha}[p_{b}sin(\alpha) - r_{b}cos(\alpha)]$$
(11)

Again, assuming turn-coordination ($\dot{\beta} = \ddot{\beta} = 0$), simplifies equation 11 into

$$\ddot{p}_s - \dot{\alpha}^2 p_s = \ddot{p}_b cos(\alpha) + \ddot{r}_b sin(\alpha) \tag{12}$$

After separating the body axis control power rates, \ddot{p}_b and \ddot{r}_b , a more intricate expression is found. Depending on the sign p_s , the acceleration build-up is either augmented or reduced with $\dot{\alpha}$. During aggressive manoeuvring initiated by the pilot, such as a rapid roll followed by a rapid load factor build-up to initiate a sharp turn, the acceleration build-up rate will decrease, necessitating a higher control power rate to sustain optimal roll performance. Furthermore, due to that the $\dot{\alpha}^2$ -term is squared, this effect persists for both roll-pull and roll-push type inputs.

By again excluding any dynamics in α , a simple expression is found for the control power rate for turn-coordinated stability axis roll acceleration build-up with constant load factor.

$$\ddot{p}_s = \ddot{p}_b cos(\alpha) + \ddot{r}_b sin(\alpha) \tag{13}$$

For a given requirement on \ddot{p}_s that satisfy a specific manoeuvre target, equations 2, 4, 10 and 13 can be combined to solve for the quantity of interest.

$$\frac{\dot{\delta}_r}{\dot{\delta}_a} = \frac{Cl_{\delta_a}}{Cn_{\delta_r}} \cdot \frac{I_z}{I_x} tan(\alpha)$$
 (14)

$$\ddot{p}_{s_{req}} = \frac{\dot{\delta}_a \cdot Q \cdot S \cdot b \cdot Cl_{\delta_a}}{I_x} cos(\alpha) + \frac{\dot{\delta}_r \cdot Q \cdot S \cdot b \cdot Cn_{\delta_r}}{I_z} sin(\alpha)$$
 (15)

For example, the required control axis deflection rate can be determined over a specified range in AoA and flight envelope (Q), provided knowledge about the control effectiveness parameters, Cl_{δ_a} , Cn_{δ_c} and the moments of inertia.

For the aircraft model considered in this paper, control axis deflection rates must be further broken down into the individual control surfaces. This is due to the control suite consisting of trailing edge flaps (elevons) and canted rudders. As such, the elevons are used for control about all axes and the rudders can be used in both pitch and yaw. Notably, the inner elevons produce substantial proverse yawing moment at high AoA.

4. Simulation Results

This section presents some analyses highlighting the effect of control power rate to augment the lateral dynamics of the aircraft. Design of control surfaces must consider several subsystem aspects such as, for instance, installation and hinge moment capability, which fall beyond the scope of this paper.

4.1 Roll performance challenges

Airframe agility refers to the capability to swiftly change both the direction and magnitude of the normal force vector, along with the time required to transition between different manoeuvring states [4]. This is particularly challenging to achieve when performing high angle of attack (AoA) turning manoeuvres at low dynamic pressure. One element of this capability is the possibility to rapidly vary the bank angle of the aircraft in order to reorient the normal force vector. However, at low dynamic pressure, changing the aircraft state will require large-amplitude deflections at high rates. Furthermore, the kinematics and inertial coupling of high AoA rolling requires all control channels to be engaged. This can lead to challenges, particularly for coupled control effectors such as elevons and canted rudders which must handle pitch, roll and yaw control simultaneously. Figure 4 illustrates the control axis deflections during a 1g roll. Some individual control surfaces are reaching maximum deflection at different times and deflecting at max rate.

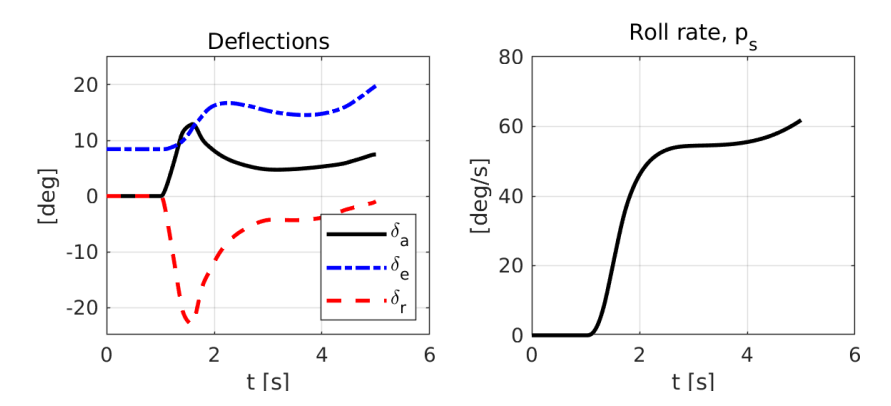


Figure 4 – Control axis deflections for a coordinated high- α roll (δ_a, δ_r) and to cancel out the inertial pitch-up effect (δ_e) .

The decline in roll performance with AoA is shown in figure 5, where a maximum deflection rate of $60^{\circ}/s$ was assumed. It is also shown that a more aft CG of the unstable platform further reduces the roll performance. This is due to that the control margin is reduced in order to trim as well as due to that the airspeed is lower for a given AoA (lower O) [5].

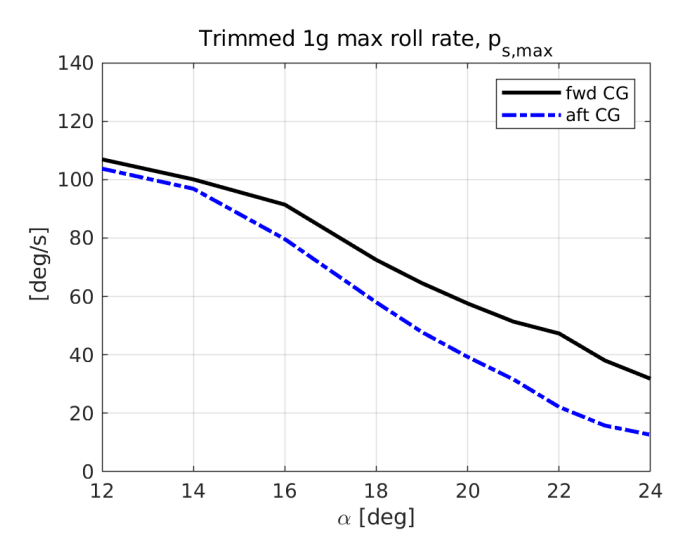


Figure 5 – Low speed roll performance.

By achieving adequate FQ/HQ within the low dynamic pressure part of the envelope, it is feasible to achieve the desired FQ/HQ throughout the flight envelope, provided that acceptable design balance can be achieved for the overall design of the aircraft. Achieving the desired FQ/HQ will, to a greater extent, become a matter of control law tuning.

4.2 Roll performance with thrust vectoring

A TVC provides propulsion control power which has different characteristics compared to aerodynamic control power from conventional control surfaces. The greatest difference comes from that the TVC is mainly dependent on the available thrust as opposed to dynamic pressure and angle of attack. Here, the thrust vectoring adds a vast amount of control power and rate in pitch and yaw, which particularly augments the manoeuvrability in low energy flight conditions where the elevons and rudders fail.

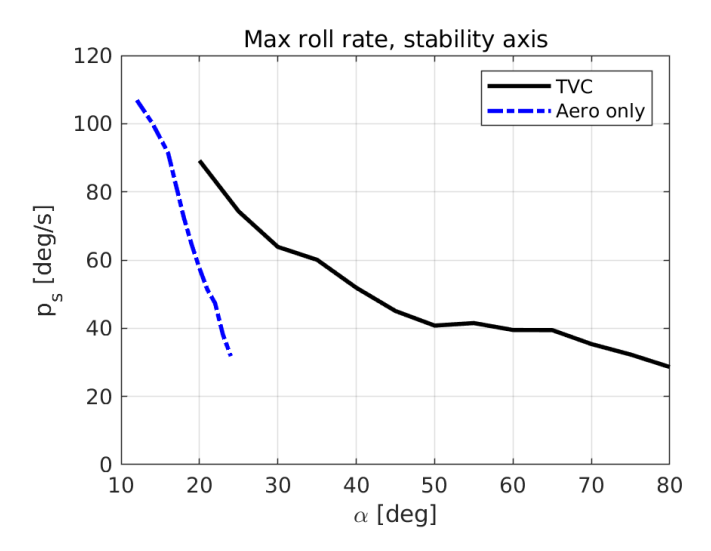


Figure 6 – Low speed roll performance with and without TVC.

Figure 6 shows that roll capability can be achieved even up to extreme angles of attack in the post-stall regime. A stability axis roll gets closer to a pure yawing motion of the airframe for very high angles of attack, as expressed by equation 5. Due to that the TVC is able to provide significant yaw and pitch control power, it is able to achieve moderate roll rates throughout the α -range whilst also maintaining longitudinal control.

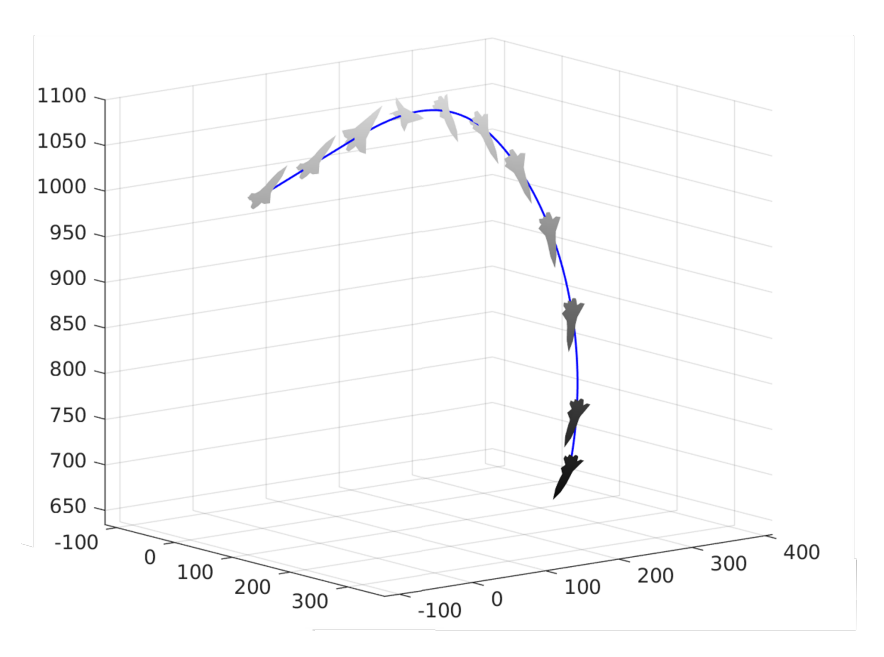


Figure 7 – Post-stall manoeuvre with thrust vectoring. The aircraft is abruptly pitched up to α =80° followed by a coordinated stability axis roll to the right.

Figure 7 illustrates a post-stall turn manoeuvre resembling a 'Herbst manoeuvre', performed at very low speed [6]. The aircraft is rapidly pitched up and then rolled to the right, achieving a swift 180° heading change.

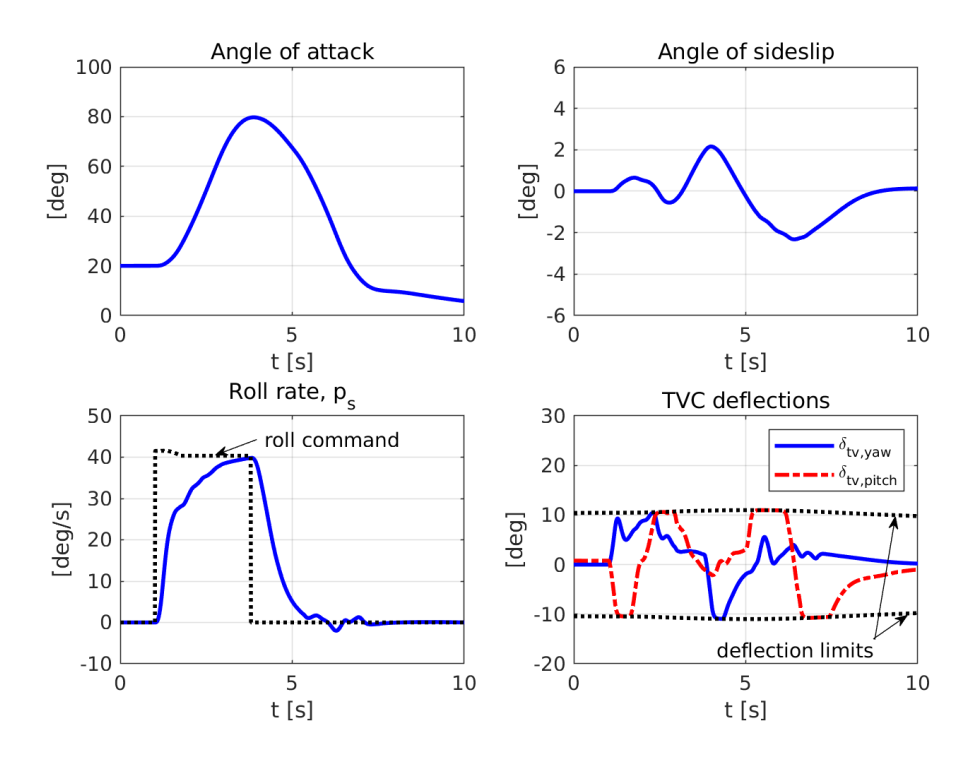


Figure 8 – Roll response and TVC deflections during a post-stall manoeuvre.

For the manoeuvre illustrated in figure 7, some times histories are plotted in figure 8. It is seen that the anlge of sideslip regulation performs reasonably well. The TVC saturates in both pitch and yaw deflection to counter the rise in pitch at very high AoA and to achieve a reasonably fast response in roll.

4.3 Roll response characteristics

For a given control surface size, the control power rate, \dot{M}_{ctrl} , is dictated by the deflection rate limit, $\dot{\delta}_{max}$, according to equation 2. Figure 9 shows the roll response following a step input in roll stick for two different limits on deflection rate. Both cases eventually converge on the same steady state roll rate. There is a greater initial lag and time delay for achieving the commanded roll for the case with the lower rate limit, see top right in figure 9.

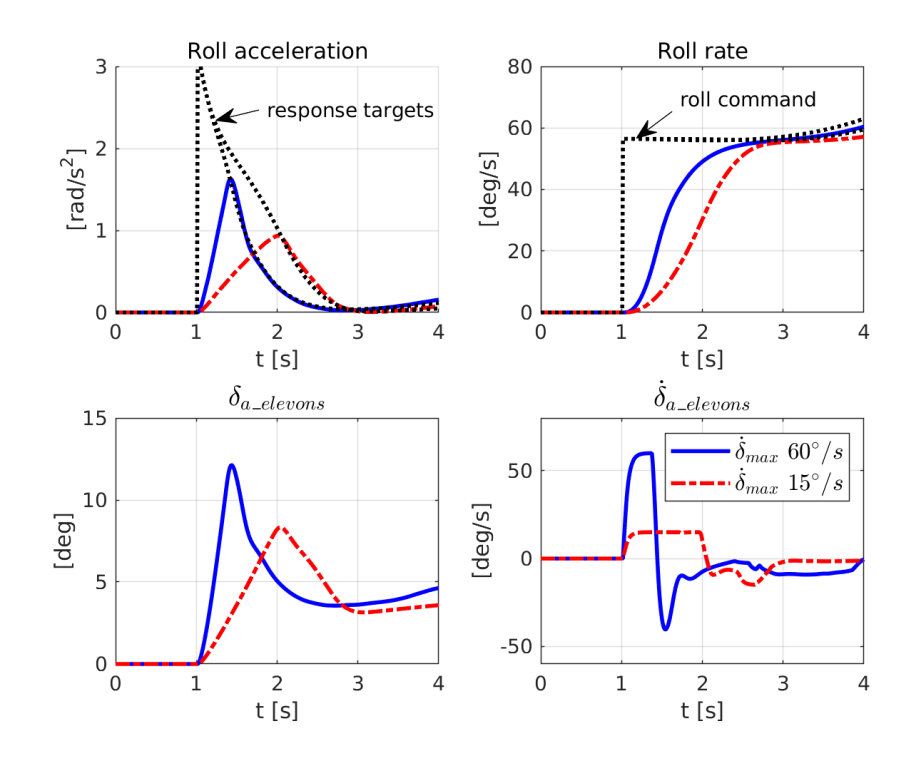


Figure 9 – Low speed roll from 1g level flight, $\alpha = 20^{\circ}$ for two different limits on deflection rate.

Response targets are calculated from the commanded roll rate and response models for which the control allocation is solved. The FCS augments the lateral dynamics by increasing the roll acceleration, i.e., decreasing the roll time constant. This is done by allocating extra control deflections - more than is required for the steady state roll, see bottom left where δ_a is the differential deflection of the elevons. For the case with the lower rate limit, the realised roll acceleration is much smaller, leading to a greater time delay in achieving the commanded roll rate.

The bottom right picture shows that saturation only occurs in deflection rate while δ_a has not reached its deflection limit. However, due to control allocation prioritisation, saturation in deflection limit does occur for some individual control surfaces. As such, the control power is limited and the available control power rate becomes more important for the achievable manoeuvre performance. This has to be synchronised with application of control power rate in the yaw control axis to coordinate the turn and keep AoS close to zero.

4.4 Roll time constant

MIL-STD-1797A specifies levels in roll time constant, τ_R , for different FQLs in roll manoeuvring for precision tasks [2]. Too high values of τ_R can cause problems where pilots, for example, are closing the loop around a roll tracking tasks such as bank angle capture. This can lead to an out-of-phase condition and by extension, may lead to a non-divergent lateral PIO.

The roll time constant is defined as the time taken to reach 63.2% of the steady state value in roll rate. For FQL 1, $\tau_R < 1s$ is the specified maximum roll time constant to achieve some steady state value in roll rate. However, lower values such as $\tau_R < .6$ -.8s have also been suggested.

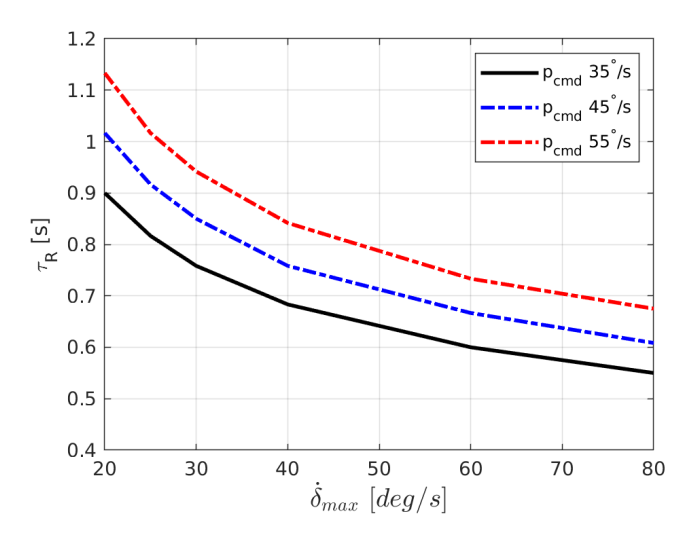


Figure 10 – Roll time constants versus max deflection rate, δ_{max} and manoeuvre authority in roll command, p_{cmd} for $\alpha = 20^{\circ}$

Figure 10 shows the roll time constants with varying control surface deflection rates and max commanded roll rate. It is not particularly demanding to satisfy $\tau_R < 1s$, within a moderate range of commanded roll rates, even for low speed flight at $\alpha = 20^\circ$. The smallest time constants are found for the lowest commanded roll rate. The implication is that in order to keep the roll time constant low, the max commanded roll rate may be reduced. Alternatively, the result show that an increase in commanded roll rate necessitates an increase in deflection rate for the same τ_R , for a given control volume. It is evident that the criterion is not particularly comprehensive for evaluating the FQ/HQ without complementing criteria.

Figure 11 shows that the roll time constant starts to deteriorate for rolling at extreme angles of attack. The plots show max roll rates, time constants and time to zero pitch angle, time-to- θ_0 ° (time taken to roll the nose down to the horizontal plane). The results are plotted for two different limits on deflection rates for all control effectors, including the TVC.

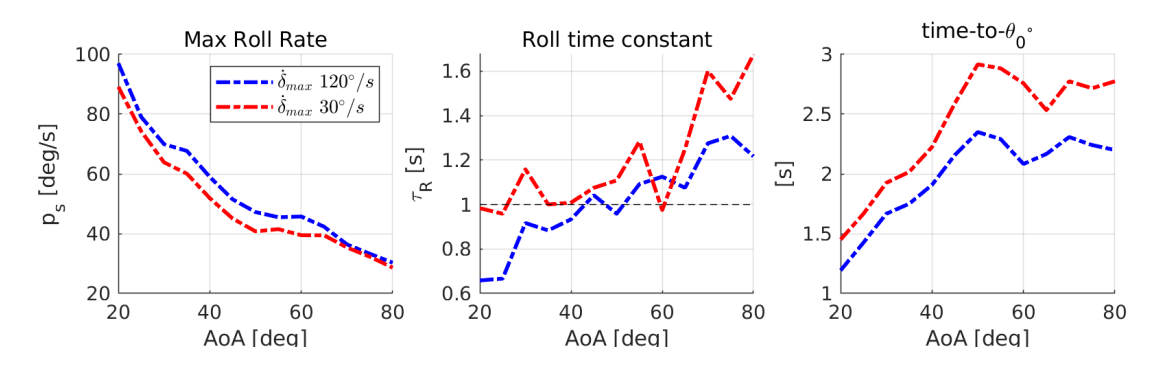


Figure 11 – Roll performance metrics for rolling at extreme angles of attack with thrust vectoring.

The roll rates represent those that can be achieved with an acceptable regulation of the sideslip angle. The decrease in roll performance is shown with decreasing roll rates and increasing roll time constants with AoA, suggesting that post-stall manoeuvring is only achieved with significantly degraded FQ/HQ. A higher value of τ_R introduces more lag in the roll response making attitude control more difficult. The case with higher rate limit shows that some additional performance is gained, which is most clearly seen for the time taken to roll the nose through the horizontal plane, i.e., 0° of pitch angle.

4.5 Roll reversals

The effect of control power rate becomes particularly evident for transient type manoeuvring such as roll reversals. For a maximum performance roll reversal, the control surfaces can be saturated in deflection limit in one direction and have to move at max rate to the limit in the opposite direction [7].

A low speed, unloaded roll reversal manoeuvre is, in itself, less relevant considering operational use. Rapid bank angle change is usually combined with loading and unloading while performing more operationally relevant manoeuvres, such as rolling scissors or displacement rolling. An additional case can include speed recovery from a low energy state in a nose-high abnormal attitude, where the energy state is more rapidly regained by rolling rather than by levelling out and pitching nose-down. However, a high- α roll reversal is a particularly demanding manoeuvre to satisfy for adequate handling. Thus, it is very exposing of the attainable level of roll manoeuvrability that can be achieved for a platform and serves as a good demonstration of the roll control capability versus design parameters.

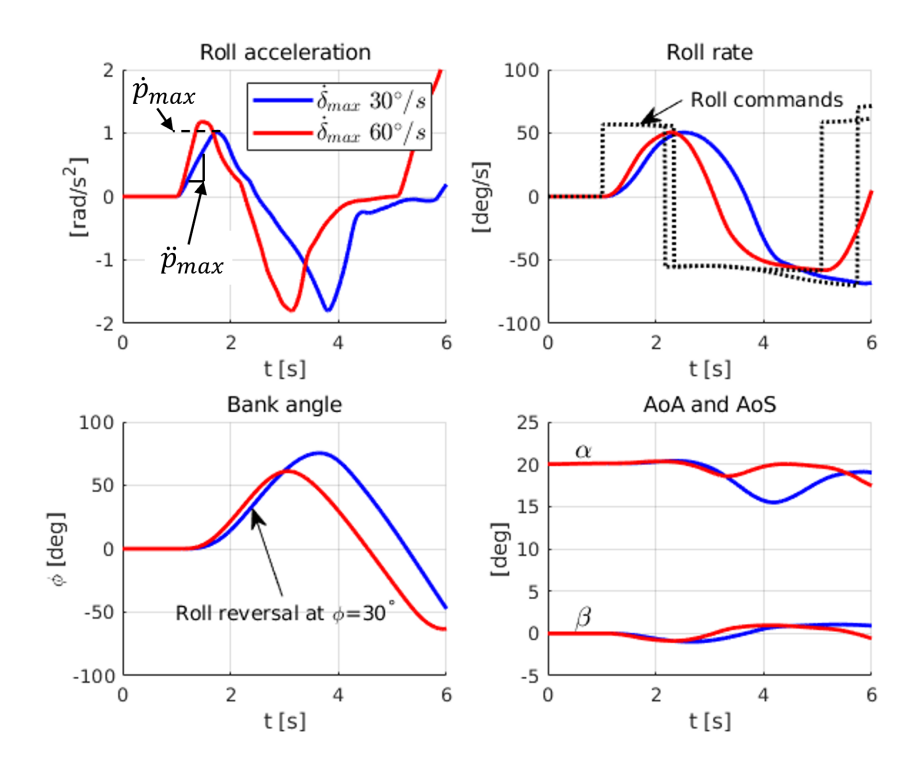


Figure 12 – Low speed roll reversal for two different limits on deflection rate.

Figure 12 shows low speed/high- α roll reversals for two different limits on deflection rate. The manoevure is performed with side-to-side step inputs in roll. The roll command is reversed when the bank angle hits +/-30 degrees, $\phi = +/-30^{\circ}$. The dotted black lines, illustrating the roll command, are shifted only due to the difference in time in achieving the bank angles.

The steady state value in roll rate is equal for both cases. The difference in peak roll acceleration, p_{max} , is predominantly due to different values in roll rate - so that the roll damping is of different magnitude - at the time when the control surfaces saturate in deflection range. In effect, the extracted control power is equally limited in both cases. The greatest difference in performance comes from that the acceleration build-up, \ddot{p}_{max} is varied. For the case with the lower deflection rate, the bank angle overshoot from $\phi=30^\circ$ is much larger due to the time taken to decelerate and accelerate the roll in the opposite direction.

To illustrate the effect of control power rate for this manoeuvre, two metrics are shown figure 13 - time-to- $\phi_{0-30-0^{\circ}}$ which is the time taken to bank to 30 degrees, reverse and pass through 0°. The

bank angle overshoot, $\Delta \phi_{ov}$, from 30 degrees of bank angle is also shown. The results are plotted versus deflection rate.

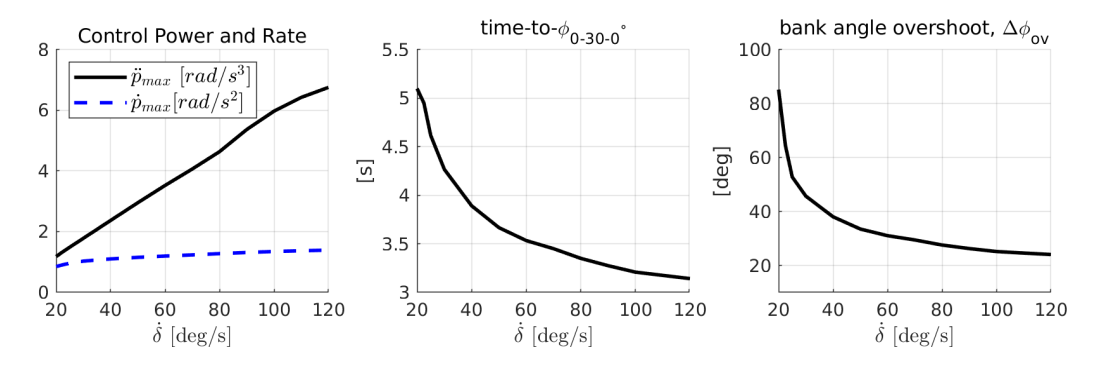


Figure 13 – Roll reversals at $\alpha=20^\circ$ for different limits on deflection rate.

In the left plot, the value of peak acceleration, \dot{p}_{max} and acceleration build-up, \ddot{p}_{max} , correspond to those depicted in figure 13, which are calculated during the initial part of the roll for each simulated case. Due to the aforementioned reason, \dot{p}_{max} , is nearly constant over the whole variation in deflection rate, $\dot{\delta}$, expect for at very low rate when deflection limit is not reached before the first reversal. As shown in the left plot, \ddot{p}_{max} increases linearly with $\dot{\delta}$.

The result gives a clear indication of the effect of control power rate. Substantial performance gain is achieved with increased fastness of the control surface rate. For instance, comparing $\dot{\delta}=30^\circ/s$ to $\dot{\delta}=90^\circ/s$, a full second has been reduced in time-to- ϕ_{0-30-0° . Additionally, even for very high deflection rates, there is a negative trend in time-to- ϕ_{0-30-0° . The bank angle overshoot results provide some insight of acceptable performance. For the low deflection rates, the overshoot is quite large which would adversely affect the pilots' opinion of the flying qualities.

4.6 Time-to-bank

Bank angle change requirements relate to the operational use for achieving necessary manoeuvring and attitude regulation. The levels specified in MIL-STD-1797A are indeed difficult to achieve for flying conditions close to V_{min} and α_{max} . However, as outlined in [2], roll performance criteria should reflect the required roll manoeuvrability at speeds that are normal for a given task. Thus, sizing criteria needs to be tailored to the specific application. Nevertheless, the roll performance criteria reproduced from MIL-STDs, shown in table 1, are used to highlight the outcome of design variation. Additionally, runs in a pilot-in-the-loop simulator with a test pilot were conducted to validate the FQLs' relevance with perceived HQ. The pilot rating confirmed the MIL-STD FQL 1 as a measure of adequate handling qualities, provided several other criteria are also met.

Table 1 – MIL-STD Flying Quality Level for time to bank angle change, very low speed range, class IV airplanes, category A

FQL vs time-to- $\phi 30^{\circ}$	
Level	[s]
1	1.1
2	1.6
3	2.6

Figure 14 shows the achieved time-to- $\phi 30^{\circ}$ for different deflection rates. Results are also shown for variation in control surface size - different values of Cm_{δ} . $Cm_{\delta} + 25\%$ signifies that the size of all control surfaces has been increased by a factor of 1.25. A scaling model is used to update each control effectiveness parameter. FQL 1 is achieved for $\dot{\delta}=105^{\circ}/s$ for the case with nominal control power, see black line, left plot. Similarly, level 1 is satisfied with $\dot{\delta}=60^{\circ}/s$ for the largest increment

in control surface size. This shows that different combinations in control surface size and deflection rate satisfy the roll criteria. The right plot shows that the roll criteria was satisfied with the same level control power rate for all three configuration. All combinations of surface size and deflection rate collapse onto the same variation in control power rate. Note that the cases with increased control effectiveness extends further giving higher values of control power rate for the same range of deflection rate variation.

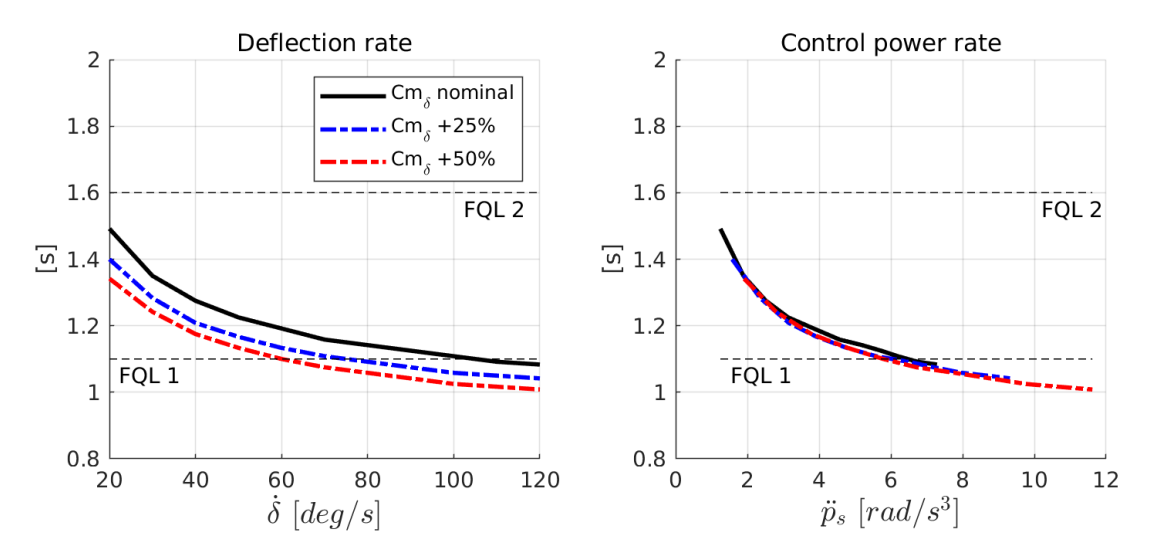


Figure 14 – Time-to- ϕ 30° at $\alpha_{max} = 20^{\circ}$.

In the right plot of figure 14, it is seen that the time-to- $\phi 30^\circ$ values cohere with one level of \ddot{p}_s , for all cases. The required control power rate is roughly equal to $\ddot{p}_s = 6 \ [rad/s^3]$ for FQL 1. However, the time-to-bank angle change is effectively the integrated roll rate w.r.t. time. The same result can, therefore, be achieved with a different combination of steady state roll rate and acceleration build-up to yield the same 'area under the curve'. This is shown in figure 15. The two cases have separate specification of manoeuvre authority and max deflection rate whilst achieving the roll criterion with equal merit. In top left plot, the dashed black lines represent the time for achieving $\phi = 30^\circ$, $t_{\phi 30}$, for both cases.

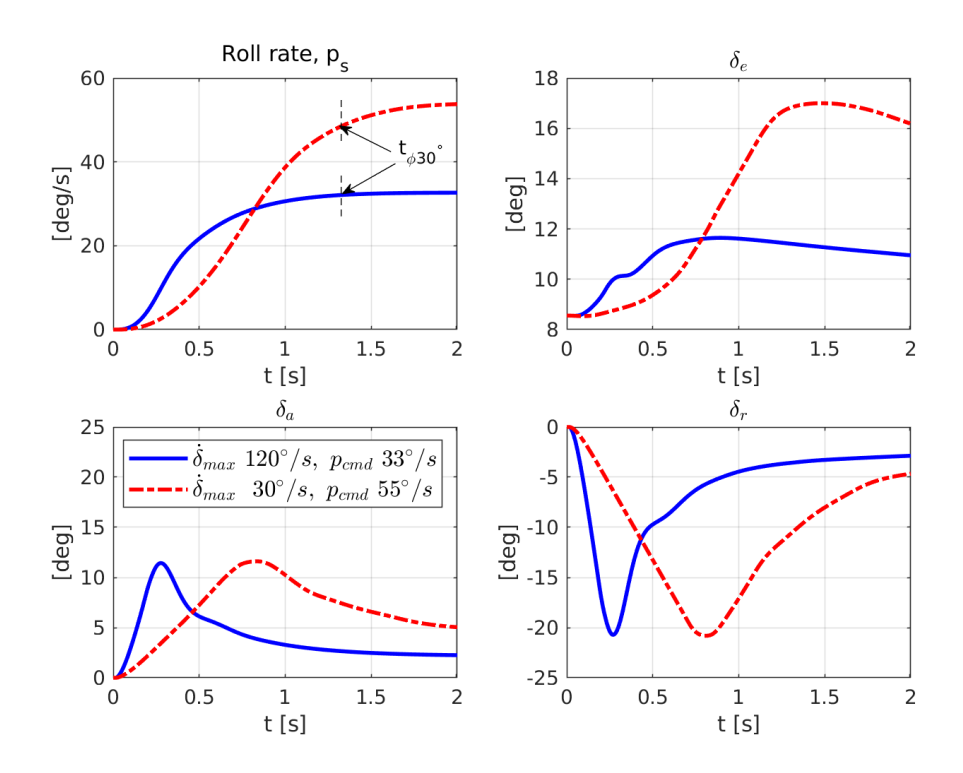


Figure 15 – Equal performance of $t_{\phi 30}$ for two cases with different combinations of max deflection rate and manoeuvre authority

It should be noted that for the case with the lower rate and higher p_{cmd} (red), the steady state value has not been achieved before $t_{\phi30}$ whilst the opposite is true for the other case. As such, the roll time constant has also increased. If the roll time constant is too high, this can lead to a potential restriction of p_{cmd} , which will be dependent on the available control power rate. This shows that several criteria need to be considered together. Other criteria, which are not included here, also need to be investigated such as, for instance, effective time delay, time in saturation, cross-coupling, local acceleration at the pilot station and control margin for pitch recovery during roll.

The different control axis deflections are shown in figure 15. Equal max deflections in roll, δ_a , and yaw, δ_r , show that the same amount of peak control power is applied for the two cases. However, in pitch, the case with the higher p_{cmd} (red), requires substantially more control power to trim out the inertial pitch-up acceleration which is due to the roll rate. With a high enough roll rate, the control surfaces will saturate in deflection and run out of pitch recovery margin. The commanded AoA and AoS are adequately achieved during the roll.

4.7 Deflection rates with thrust vectoring

During turning manoeuvres at high AoA or at low dynamic pressure, within the nominal flight envelope, the required thrust is typically high to sustain flight. Thus, the TVC is able to significantly augment the lateral dynamics.

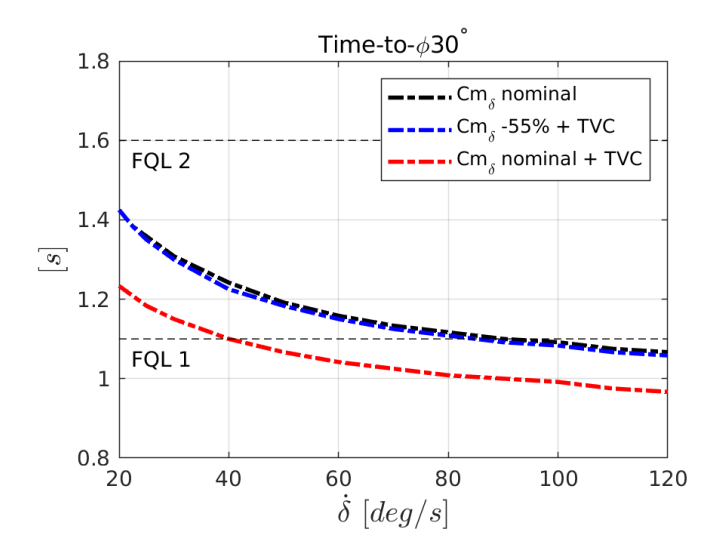


Figure 16 – Time-to- $\phi 30^{\circ}$ with thrust vectoring.

Figure 16 shows the time-to- $\phi 30^\circ$, comparing the performance of TVC with aerodynamic control surfaces versus aerodynamic control surfaces only. Additionally, a third case illustrate the possible reduction in control power of the aerodynamic control surfaces for the same roll performance. A substantial decrease in the required rates is shown for the combined control suite when adding TVC. The TVC lowers the required deflection rate of all control effectors to satisfy the FQL 1 criterion.

4.8 Combining several roll performance criteria

Recalling that equations 14 and 15 can be used with a specification of the required control power rate, $\ddot{p}_{s_{req}}$, that satisfy manoeuvre targets for a stability axis roll. Here, the aforementioned criteria are combined such that $\ddot{p}_{s_{req}}$ can be found that satisfy all.

In figure 17, the required control power rate, $\ddot{p}_{s,req}$ is plotted as a function of manoeuvre authority in roll rate command, time-to- $\phi 30^{\circ}$ and roll time constant is also included. For demonstration purposes, selected criteria include:

- $t_{\phi 30^{\circ}} < 1.3s$
- $\tau_R < 0.8s$
- $p_{s,min} > 40^{\circ}/s$

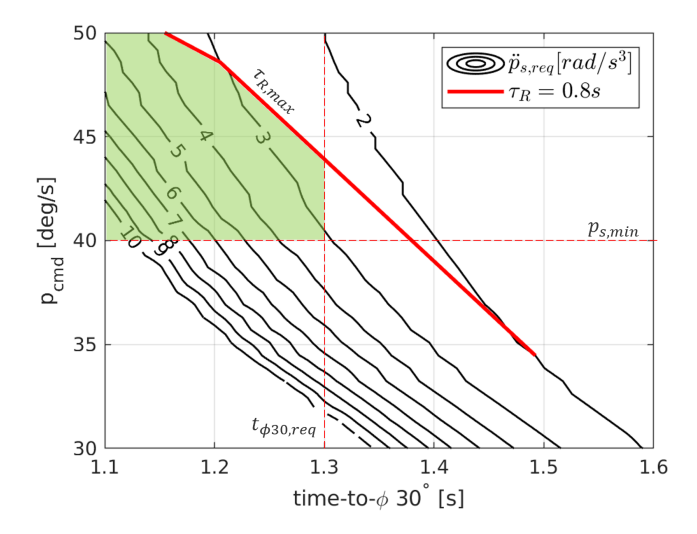


Figure 17 – Combining several requirements - required control power rate versus time-to- ϕ 30°, roll time constant, $\tau_R = 0.8$, and manoeuvre authority, p_{cmd} , at $\alpha = 20^\circ$.

The range of $\ddot{p}_{s,req}$ represent those that can be achieved within a range of reasonable max deflection rates, $(20 < \dot{\delta}_{max} < 120^{\circ}/s)$. Using the above-stated criteria, the intersection of those constrains the available design space. These are drawn such that the remaining design space can be isolated (see the green shaded area). An upper limit roll rate can be chosen for a minimum control power rate requirement or vice versa.

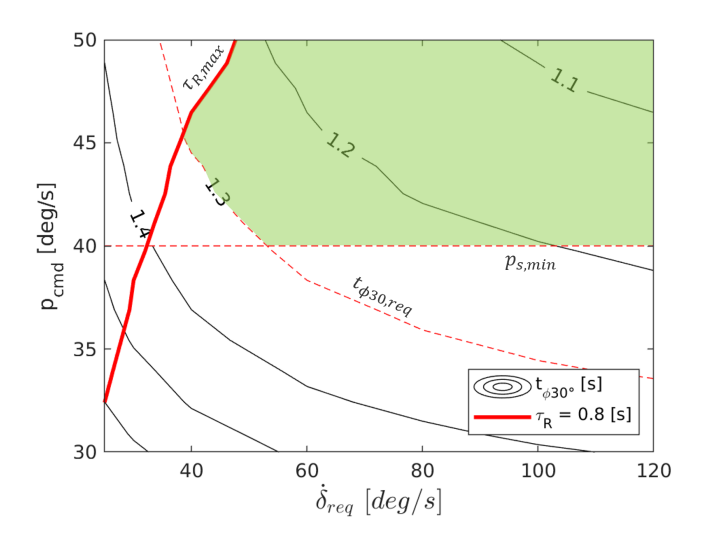


Figure 18 – Combining several requirements - time-to- ϕ 30° and roll time constant, $\tau_R = 0.8$, versus control surface deflection rate and manoeuvre authority, p_{cmd} , for a given control effectiveness.

The result in figure 18 is produced to express the max required deflection rates instead of control power rate using the above-stated criteria. This is done for a given control power, corresponding to " Cm_{δ} nominal" in figure 14. With a specific p_{cmd} of 45deg/s, the lowest required deflection rate is found so that $\dot{\delta}_{req}$ is roughly 40deg/s to satisfy all criteria. For stricter constraints of the time-to-bank criterion, there is a dramatic increase in the required deflection rate. It should be noted, that by increasing the maximum deflection range of a control surface to extract additional control moment, it will also require higher deflection rate limits to be useful for augmenting the FQ/HQ. This is due to that the maximum control potential must be reached within the same amount of time.

5. Conclusions

To achieve high manoeuvre performance in unstable aircraft, it is essential to ensure proper stabilisation, agility and superior flying and handling qualities. Traditional sizing methods for control power seldom include the aspects of control power rate for FQ/HQ. Sizing of control power rate is critical for ensuring excellent FQ/HQ and necessitates a sizing approach that allows sufficiently rapid manoeuvre onset, precision tracking and attitude control. While handling qualities evaluation needs to be performed with pilot-in-the-loop simulators or flight tests, certain flying qualities metrics can be used and combined that will cater for the possibility to achieve excellent FQ/HQ. The flight dynamics analysis has been performed using an NDI-based FCS for a specific fighter concept. The impact of control power rate has been explored with a focus on high angle of attack roll performance. The evaluation was performed by assessing achievable FQLs defined by MIL-STD design guidance criteria.

The importance of control power rate becomes particularly significant during dynamic manoeuvring or when the available control power is limited, such as achieving rapid transient response at the edge of the flight envelope. Analyses show that the control power rate provided by a combination of control volume and control surface deflection rate needs to be tailored to satisfy several manoeuvre targets. The addition of thrust vectoring adds considerable control power and rate such that the aerodynamic control surfaces can be significantly reduced in size and/or deflection rate for the same roll performance. Furthermore, particularly demanding post-stall manoeuvres have been demonstrated with the use of thrust vectoring, although with a degradation in roll response qualities.

6. Contact Author Email Address

mailto: philip.mansson@saabgroup.com

7. Copyright Statement

The author confirms that he, and/or his company or organization, hold copyright on all of the original material included in this paper. The author also confirms that they have obtained permission, from the copyright holder of any third party material included in this paper, to publish it as part of their paper. The author confirms that he gives permission, or has obtained permission from the copyright holder of this paper, for the publication and distribution of this paper as part of the ICAS proceedings or as individual off-prints from the proceedings.

References

- [1] Kay J, Mason W., Durham W., Lutze F., Benoliel A. Control Authority Issues in Aircraft Conceptual Design: Critical Conditions, Estimation Methodology, Spreadsheet Assessment, Trim and Bibliography. VPI-Aero-200. 1996.
- [2] Flying Qualities of Piloted Aircraft, MIL-STD-1797A. Aeronautical Systems Center, Wright-Patterson AFB, OH, June 1995.
- [3] Marilyn E, Ogburn, John V. Foster, Joseph W. Pahle, R. Joe Wilson, James B. Lackey,. *Status of the Validation of High-Angle-of-Attack Nose-Down Pitch Control Margin Design Guidelines*. AIAA paper 93-3623, August 1993.
- [4] Skow M. A. *Agility as a contributor to design balance*. AIAA/SFTE/DGLR/SETP Fifth Biannual Flight Test Conference, Ontario, CA, 1990.
- [5] Johansson E., Månsson P., Sjöberg P., Flight Dynamics Simulation and FCS auto-generation in the conceptual design phase of unstable supersonic aircraft. ICAS 33rd Conference, Stockholm, 2022.
- [6] Robinson M.R., Herbst W.B. *The X-31A and Advanced Highly Maneuverable Aircraft.* 17th ICAS Congress, Stockholm, Sweden, 1990, Proceedings Vol. I, pp. LV-LXIV
- [7] Dorsett K., Mehl D, Innovative control effectors (ICE). Defence Technical Information Center, 1996.